Cancer Cell
Article

Mouse Model of Human Ovarian Endometrioid Adenocarcinoma Based on Somatic Defects in the Wnt/β-Catenin and PI3K/Pten Signaling Pathways

Rong Wu,[1,9] Neali Hendrix-Lucas,[1,9] Rork Kuick,[2] Yali Zhai,[1] Donald R. Schwartz,[1,10] Aytekin Akyol,[3] Samir Hanash,[4] David E. Misek,[5] Hidetaka Katabuchi,[7] Bart O. Williams,[8] Eric R. Fearon,[1,2,3,6] and Kathleen R. Cho[1,2,3,*]

[1] Department of Pathology
[2] Comprehensive Cancer Center
[3] Department of Internal Medicine
[4] Department of Pediatrics and Communicable Diseases
[5] Department of Surgery
[6] Department of Human Genetics
University of Michigan Medical School, Ann Arbor, MI 48109, USA
[7] Department of Gynecology, Faculty of Medical and Pharmaceutical Sciences, Kumamoto University, Kumamoto 860-8556, Japan
[8] Van Andel Research Institute, Grand Rapids, MI 49503, USA
[9] These authors contributed equally to this work.
[10] Present address: Biodiscovery LLC, 3886 Penberton Drive, Ann Arbor, MI 48109, USA.
*Correspondence: kathcho@umich.edu
DOI 10.1016/j.ccr.2007.02.016

SUMMARY

One histologic subtype of ovarian carcinoma, ovarian endometrioid adenocarcinoma (OEA), frequently harbors mutations that constitutively activate Wnt/β-catenin-dependent signaling. We now show that defects in the PI3K/Pten and Wnt/β-catenin signaling pathways often occur together in a subset of human OEAs, suggesting their cooperation during OEA pathogenesis. Deregulation of these two pathways in the murine ovarian surface epithelium by conditional inactivation of the *Pten* and *Apc* tumor suppressor genes results in the formation of adenocarcinomas morphologically similar to human OEAs with 100% penetrance, short latency, and rapid progression to metastatic disease in upwards of 75% of mice. The biological behavior and gene expression patterns of the murine cancers resemble those of human OEAs with defects in the Wnt/β-catenin and PI3K/Pten pathways.

INTRODUCTION

The vast majority of primary ovarian cancers are carcinomas, since they show epithelial differentiation. It is widely believed that ovarian carcinomas usually arise from the ovarian surface epithelium (OSE) or from surface epithelial inclusion glands and cysts. Endometriosis is also considered a plausible and well-documented, but not necessarily obligate, precursor of ovarian carcinomas, particularly those with clear cell or endometrioid differentiation (Campbell and Thomas, 2001; Bell, 2005). Pathologists currently employ a classification system for ovarian carcinomas based entirely on light microscopic analysis of tumor cell morphology (Scully et al., 1998). At least some of the morphological heterogeneity of ovarian carcinomas may be due to aberrant expression of *HOX* genes, which

SIGNIFICANCE

Ovarian carcinomas can be subclassified into four major types (serous, endometrioid, clear cell, and mucinous) based on their morphological features. Here, we demonstrate that mutations of the Wnt/β-catenin and PI3K/Pten signaling pathways cooperate in the development of ovarian endometrioid adenocarcinomas in women and in mice. Our mouse model of ovarian cancer, based on conditional deletion of *Apc* and *Pten*, shows morphological features, biological behavior, and gene expression profiles similar to human cancers with the same signaling pathway defects. This model should help advance understanding of the pathogenesis of human ovarian cancer and will likely prove useful for preclinical testing of therapies targeting the Wnt/β-catenin and PI3K/Pten signaling pathways.

regulate Müllerian duct differentiation and specify morphological identity within the female reproductive tract (Cheng et al., 2005). The present clinical management of a given ovarian cancer is not significantly influenced by its morphological subtype (serous, endometrioid, clear cell, or mucinous) (Guppy et al., 2005), though a substantial body of molecular data indicate that the different subtypes are generally characterized by distinct genetic alterations (Bell, 2005). For example, about 85% of mucinous ovarian adenocarcinomas harbor *K-RAS* gene mutations, while *K-RAS* mutations are much less frequently observed in clear cell, endometrioid, and typical (high-grade) serous carcinomas (Ichikawa et al., 1994; Cuatrecasas et al., 1997; Enomoto et al., 1991). Likewise, mutations of the *CTNNB1* gene (encoding β-catenin) are observed in 16%–38% of ovarian endometrioid adenocarcinomas (OEAs) but are uncommon in the other types of ovarian carcinomas (Gamallo et al., 1999; Sagae et al., 1999; Wright et al., 1999; Wu et al., 2001; Kildal et al., 2005; Catasus et al., 2004). As in other cancers, the genes mutated in ovarian cancer typically encode proteins that function in conserved signaling pathways (Vogelstein and Kinzler, 2004). A better understanding of how the pathway defects cooperate in a given tumor should allow molecularly targeted therapies to be developed and implemented in the future.

Genetically engineered mouse (GEM) models of each major subtype of ovarian cancer will undoubtedly prove useful for improving knowledge of ovarian cancer biology and for preclinical testing of signal transduction inhibitors as therapeutics. Historically, most animal models of ovarian cancer were based on xenografting human ovarian cancer cells into immunodeficient mice. Such models have limitations, including incomplete recapitulation of tumor-host interactions and inability to replicate early stages of tumor development. Recently described GEM models of ovarian cancer address some limitations of the xenograft models. Most of the GEM models described thus far result in tumors most closely resembling human ovarian serous carcinomas (Flesken-Nikitin et al., 2003; Orsulic et al., 2002; Connolly et al., 2003). Another GEM model, involving conditional deletion of *Pten* and activation of an oncogenic *K-ras* allele in the ovarian surface epithelium, results in tumors with apparent morphological similarity to human OEAs (Dinulescu et al., 2005). However, *K-RAS* mutations have been reported in less than 10% of human OEAs (Sieben et al., 2004; Amemiya et al., 2004; Caduff et al., 1998; Enomoto et al., 1991), and data supporting cooperation between K-Ras mutation and Pten inactivation in human OEAs are lacking.

Here, we report that activation of PI3K/Pten signaling on the basis of *PTEN* inactivation and/or *PIK3CA* mutation is significantly associated with canonical Wnt (Wnt/β-catenin/Tcf, hereafter referred to as Wnt/β-cat) signaling pathway defects in a subset of human OEAs. The OEAs with deregulated Wnt/β-cat and/or PI3K/Pten signaling tended to be low grade, and unlike high-grade OEAs, uncommonly had p53 mutations. This distinction is a major source of gene expression variation in OEAs. Notably, *K-RAS* mutations were not observed in tumors with Pten inactivation. Deregulation of PI3K/Pten and Wnt/β-cat signaling in the murine ovarian surface epithelium was achieved by conditional deletion of the *Pten* and *Apc* tumor suppressor genes, respectively, and resulted in tumors with similar morphology, biological behavior, and gene expression patterns to human OEAs with the same signaling pathway defects. This model of ovarian cancer should allow further study of ovarian cancer biology in an in vivo setting and will likely prove useful for preclinical testing of Wnt/β-cat and PI3K/Pten signal transduction inhibitors.

RESULTS

Mutations of *PTEN* Are Frequently Observed in Human OEAs with Mutant β-Catenin, but Not in OEAs with Mutant K-Ras

Previous studies have shown the canonical Wnt (i.e., Wnt/β-catenin/Tcf) signaling pathway is deregulated in 16%–38% of human OEAs (Wright et al., 1999; Sagae et al., 1999; Moreno-Bueno et al., 2001). In our series of 72 primary OEAs, 18 had missense mutations of *CTNNB1*, and 1 was found to harbor inactivating mutations in both alleles of the *APC* tumor suppressor gene. Hence, in keeping with published data from others, 26% of our primary OEAs have mutations predicted to deregulate Wnt/β-cat signaling. Based on immunohistochemical staining of tumor tissue (data not shown), nuclear accumulation of β-catenin protein was observed, as expected, in a comparable percentage of OEAs (21 of 72) and included 18 samples with *CTNNB1* or *APC* mutations (see Table S1 in the Supplemental Data available with this article online). β-catenin mutation and immunohistochemistry data from a subset of these OEAs have been reported earlier (Wu et al., 2001; Zhai et al., 2002).

Inactivating mutations of the tumor suppressor gene *PTEN* have been reported in 14%–21% of OEAs but are rare in the other types of ovarian carcinomas (Obata et al., 1998; Catasus et al., 2004). Inactivation of Pten, the lipid phosphatase that converts PIP3 to PIP2, is one mechanism by which activation of phosphotidylinositol 3-kinase (PI3K) signaling occurs in human tumors (reviewed by Altomare and Testa, 2005). In order to determine whether defects of the Wnt/β-cat and PI3K/Pten signaling pathways co-occur in OEA pathogenesis, we sequenced all nine *PTEN* exons in our collection of 72 primary OEAs previously characterized for mutations of Wnt/β-cat pathway genes. Nonsense, frameshift, or missense *PTEN* mutations were identified in 8 of the 72 tumors (Table 1). Several lines of evidence support the functional significance of the four missense *PTEN* mutations we identified. First, amino acid changes at the same position of each missense mutation have been reported (http://www.sanger.ac.uk/genetics/CGP/cosmic/), and one of these, R130G, affects the codon most frequently mutated in human cancers. Moreover, all four missense mutations are in exon 5, which encodes the phosphatase domain of the Pten protein, and there are several reports in the published literature showing the functional significance of

Table 1. Mutational Analysis of *PTEN* and Corresponding Mutations of *CTNNB1* and K-*RAS* in OEAs

Tumor ID	*PTEN* Mutation (Exons 1–9)	*CTNNB1* Mutation (Exon 3)	K-*RAS* Mutation (Codons 12 and 13)
OE-13T	del T, exon 4, frameshift	TCT→TGT	none
OE-19T	GAG→TAG, exon 1, nonsense	TCT→TAT	none
OE-31T	TAT→AAT, exon 5 (Tyr→Asn)	none	none
OE-48T	ACT→CCT, exon 5 (Thr→Pro)	GGA→GAA	none
OE-54T	ACG→AGG, exon 5 (Thr→Arg)	GAC→GCC	none
OE-55T	del ACTT, exon 8, frameshift	TCT→TTT	none
OE-63T	CAG→TAG, exon 6, nonsense	none	none
OE-75T	GAT→GGT, exon 5 (Gly→Asp)	none	none

such missense mutations, including loss or reduction of phosphatase activity and increased phosphorylation of Akt (Han et al., 2000; Kato et al., 2000). Comparable to other tumor types with activation of the PI3K signaling pathway due to *PTEN* inactivation (Thomas et al., 2004; Baeza et al., 2003), OEAs with mutant *PTEN* showed marked reduction or loss of Pten protein and increased expression of pS6, an indicator of PI3K pathway activation, based on immunohistochemical staining of tumor tissue (data not shown). Notably, five of the eight OEAs with mutant *PTEN* also harbored mutations of *CTNNB1.* Overall, 5 of 19 (26%) primary OEAs with deregulated Wnt/β-cat signaling also had mutations of *PTEN*. In contrast, only 3 of 53 (6%) primary OEAs lacking Wnt/β-cat signaling pathway defects had *PTEN* mutations. The association of *PTEN* mutations with Wnt/β-cat pathway defects in OEAs is statistically significant ($p = 0.026$, two-sided Fisher's exact test). All 72 OEAs were also evaluated for the presence of *K-RAS* mutations at codons 12 and 13. Although *K-RAS* mutations were identified in 5 of the 72 OEAs (7%; all in codon 12), none of the OEAs with *PTEN* mutation harbored a *K-RAS* mutation. Only 1 of 19 OEAs with Wnt/β-cat pathway defects had mutant *K-RAS*. The low frequency of *K-RAS* mutations in our series of OEAs is in accord with several studies in the published literature, which report *K-RAS* mutations in less than 10% of OEAs (Caduff et al., 1998; Enomoto et al., 1991; Sieben et al., 2004; Amemiya et al., 2004).

PIK3CA, which Encodes the p100α Catalytic Subunit of PI3K, Is Mutated in a Subset of OEAs

Recently, Oda and colleagues reported a high frequency of concomitant mutations of *PIK3CA* and *PTEN* in uterine endometrioid adenocarcinomas (UEAs) (Oda et al., 2005). Their mutational analysis of *PIK3CA* was restricted to exons 9 and 20 because most previously reported *PIK3CA* mutations in other tumor types are clustered in these regions (Samuels et al., 2004). Functional studies suggested that mutation of both *PIK3CA* and *PTEN* may have an additive effect on PI3K pathway activation. Given the findings in UEAs, we sequenced exons 9 and 20 in our 72 primary OEAs. We identified five OEAs with *PIK3CA* mutations (Table 2), a somewhat lower frequency (7%) than previously reported by Campbell and colleagues, who identified *PIK3CA* mutations in 20% of ovarian endometrioid and clear cell carcinomas but in only 6% of ovarian carcinomas when all types were considered (Campbell et al., 2004). Notably, however, all five OEAs with *PIK3CA* mutations also harbored mutations in *PTEN* ($n = 2$), *CTNNB1* ($n = 2$), or both ($n = 1$). Overall, of the ten OEAs with PI3K/Pten pathway defects (i.e., *PTEN* and/or *PIK3CA* mutations), seven (70%) also had Wnt/β-cat pathway defects, whereas of the remaining 62 OEAs sequenced for both *PIK3CA* and *PTEN* that showed no mutations, only 12 (19%) had Wnt/βcat pathway defects ($p = 0.002$, two-sided Fisher's exact test). Taken together, our findings imply that Wnt/β-cat and PI3K/Pten signaling pathway defects often cooperate in human OEA pathogenesis, while defects in K-Ras and the PI3K/Pten pathway do not. This is not necessarily the case in UEAs, which have a higher prevalence of both *K-RAS* mutations (13%–26%) (Caduff et al., 1998) and *PTEN* mutations (37%–61%) (Tashiro et al., 1997; Risinger et al., 1998). Indeed, concurrent *K-RAS* and *PTEN* mutations were recently reported in 3 of 24 complex endometrial hyperplasias, precursors of UEAs (Brachtel et al., 2005). In keeping with

Table 2. Mutational Analysis of *PIK3CA* and Corresponding Mutations of *PTEN* and *CTNNB1* in OEAs

Tumor ID	*PIK3CA* Mutation	*PTEN* Mutation	*CTNNB1* Mutation
OE-21T	H1047R, exon 20	none	GGA→GAA (Gly34Glu)
OE-31T	H1047R, exon 20	TAT→AAT, exon 5 (Tyr→Asn)	none
OE-55T	E542K, exon 9	del ACTT, exon 8, frameshift	TCT→TTT (Ser37Phe)
OE-71T	E542K, exon 9	none	GGA→GAA (Gly34Glu)
OE-75T	H1047R, exon 20	GAT→GGT, exon 5 (Gly→Asp)	none

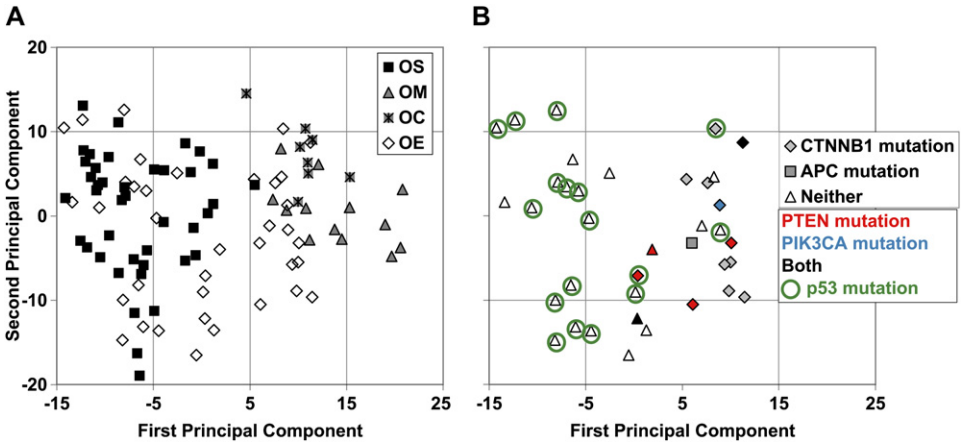

Figure 1. Gene Expression Profiling of Human Ovarian Carcinomas

(A) Principal component analysis of 99 ovarian carcinomas using all probe sets on the U133A array; the first two principal components are shown. Individual tumors are annotated with histological type as indicated (OC, clear cell; OE, endometrioid; OM, mucinous; OS, serous).

(B) Same scatter plot showing only the locations of OEAs, annotated with mutational status of *CTNNB1*, *APC*, *PTEN*, *PIK3CA*, and *p53* as indicated.

other data in the published literature, our OEAs with mutations predicted to deregulate the Wnt/β-cat and PI3K/Pten pathways tended to be low-grade, low-stage tumors. Of 44 stage 1 and 2 tumors, 21 had mutations of *CTNNB1*, *APC*, *PTEN*, and/or *PIK3CA*, while only 1 of 28 higher-stage tumors had such mutations ($p = 5 \times 10^{-5}$). Similarly, 14 of 18 grade 1 tumors versus 7 of 54 higher-grade tumors had *PTEN*, *PIK3CA*, *APC*, and/or *CTNNB1* mutations ($p = 7 \times 10^{-7}$). Clinical and molecular data associated with the group of 72 OEAs are provided as Supplemental Data (Table S1).

p53 Mutations Are Uncommon in OEAs with Wnt/β-Catenin or PI3K/Pten Pathway Defects but Are Common in High-Grade OEAs

Previous studies have reported p53 mutations in upwards of 60% of OEAs, particularly in high-grade tumors (Kolasa et al., 2006). We sequenced *TP53* exons 5–8 in all 72 OEAs and performed immunohistochemical staining for p53 protein in all but three samples. p53 mutations were documented in 32 of 72 OEAs (Table S1); five additional OEAs showed diffuse and strong nuclear accumulation of p53 protein, presumably because of a missense mutation outside of the exons sequenced. Of the 18 grade 1 OEAs, only 3 had documented or presumptive p53 mutations. In contrast, p53 mutations were identified in 34 of 54 higher-grade (2 or 3) tumors ($p = 0.0009$, two-sided Fisher's exact test). Moreover, we found documented or presumptive p53 mutations in only 2 of 22 OEAs with Wnt/β-cat and/or PI3K/Pten signaling defects, but p53 mutations were present in 35 of 50 OEAs lacking defects in these pathways ($p = 1.5 \times 10^{-6}$). Our findings support the division of OEAs into two subgroups. One group of OEAs is characterized by mutations that deregulate the canonical Wnt/β-cat and PI3K/Pten signaling pathways. These tumors typically lack p53 mutations and are low grade (grade 1), whereas a second group of OEAs harbor mutations of p53 without Wnt/β-cat or PI3K/Pten deregulation and tend to be high grade (grade 2 or 3).

We previously used Affymetrix HuGeneFL (7069 probe sets) oligonucleotide microarrays to profile gene expression in 104 primary ovarian carcinomas including all four major histological types (Schwartz et al., 2002). We showed that mucinous and clear cell carcinomas were readily distinguishable from serous carcinomas based on their gene expression profile. In contrast, OEAs showed substantial overlap with the other types. We have performed a similar gene expression analysis of 99 primary ovarian carcinomas (see Table S2 for details; 37 endometrioid, 41 serous, 13 mucinous, and 8 clear cell carcinomas, including 71 from the earlier study) using higher-density (22,283 probe sets) U133A arrays. Principal component analysis of log-transformed data was employed to provide a visual depiction of the variation in gene expression among the 99 human tumors (Figure 1A). Principal components were computed utilizing all probe sets on the arrays. Even in this unsupervised analysis, the serous, clear cell, and mucinous carcinomas are largely separable from each other. In contrast, the OEAs are rather dispersed, with several overlapping the region occupied by serous carcinoma samples, and a few close to clear cell and mucinous carcinoma samples. When the gene expression data for the OEAs are annotated with the mutational status of p53 and the Wnt/β-cat and PI3K/Pten signaling pathways (Figure 1B), it becomes evident that OEAs with p53 mutations are those with greatest overlap to the serous carcinomas and are largely distinct from OEAs with Wnt/β-cat and/or PI3K/Pten signaling pathway defects. Notably, p53 mutations have been reported in upwards of 60% of serous carcinomas, but in only 16% and 10% of mucinous and clear cell carcinomas, respectively (Schuijer and Berns, 2003).

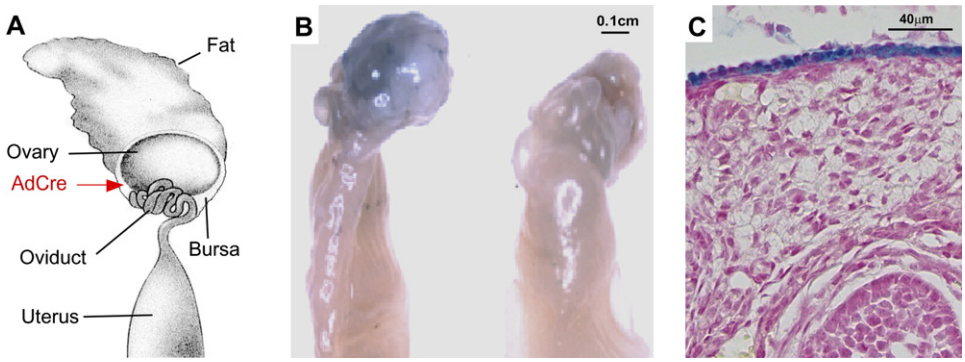

Figure 2. Ovarian Bursal Injection of AdCre Results in Ovarian Surface Epithelial Expression of Cre Recombinase

(A) Schematic diagram of ovarian bursal AdCre injection strategy (modified from Nagy et al., 2003).

(B) Whole-organ staining of β-galactosidase in the mouse oviduct and ovary following AdCre injection (left) compared to control uninjected ovary (right).

(C) Photomicrograph showing histochemical detection of LacZ in the ovarian surface epithelium. Note the absence of staining in the underlying gonadal stromal and follicular cells.

Deregulation of the Wnt/β-Catenin and PI3K/Pten Signaling Pathways in the Murine Ovarian Surface Epithelium Induces Tumors with Similar Biological Behavior and Morphology to Human OEAs

In light of our data identifying co-occurrence of Wnt/β-cat and PI3K/Pten signaling defects in human ovarian endometrioid tumorigenesis, we wished to determine whether deregulation of these two pathways in the murine ovarian surface epithelium (MOSE) induces endometrioid-like ovarian tumors in mice. In order to achieve this, we employed the method described by Flesken-Nikitin et al. and Dinulescu et al. to inactivate the *Pten* and *Apc* tumor suppressor genes in the MOSE (Flesken-Nikitin et al., 2003; Dinulescu et al., 2005). Replication-deficient adenovirus expressing Cre recombinase (AdCre) was first injected into the ovarian bursa (Figure 2A) of *Gt(ROSA)26Sor* reporter mice to verify delivery of the adenovirus to the MOSE. As expected, after staining for β-galactosidase activity using standard protocols, visual inspection of the ovary revealed blue staining (Figure 2B), which was localized to the MOSE in frozen sections (Figure 2C). We obtained the $Pten^{loxP/loxP}$ transgenic mice developed by T. Mak and colleagues (University Health Network, University of Toronto) in which Cre-mediated recombination results in deletion of *Pten* exons 4 and 5 (Suzuki et al., 2001). We also obtained the $Apc^{loxP/loxP}$ transgenic mice developed by T. Noda and colleagues (The Cancer Institute, Tokyo, Japan) (Shibata et al., 1997). In these animals, Cre-mediated recombination deletes a region of *Apc* encompassing exon 14 and induces a frameshift mutation at codon 580. The $Pten^{loxP/loxP}$ and $Apc^{loxP/loxP}$ mice were crossed to generate $Apc^{loxP/loxP}Pten^{loxP/loxP}$ mice. At 8–10 weeks of age, AdCre was injected into the right ovarian bursa of 50 $Apc^{loxP/loxP}Pten^{loxP/loxP}$ females. A subset of mice (n = 29) was followed to assess the natural history of tumor progression. Tumors (hereafter referred to as $APC^{-}/PTEN^{-}$ tumors) developed in the AdCre injected ovary with 100% penetrance (Figure 3A). Tumors were grossly apparent within 6 weeks of AdCre injection (Figure 3B), and animals died or were euthanized per guidelines for the humane treatment of animals within 19 weeks after AdCre injection (range 7–19 weeks, average 11.5 weeks). The mouse tumors pursued a course similar to untreated human ovarian carcinoma, with 76% of animals developing hemorrhagic ascites (Figure 3C), and a smaller subset (21%) developing overt peritoneal dissemination. Once established, tumor volume doubled roughly every 3 weeks (Figure 3D). A survival curve for the cohort of 29 AdCre-injected $Apc^{loxP/loxP}Pten^{loxP/loxP}$ mice is provided in Figure 3E. To date, we have not identified ovarian tumor formation in any of 33 wild-type, 61 $Apc^{loxP/loxP}$, or 63 $Pten^{loxP/loxP}$ mice following ovarian bursal injection with AdCre (surveillance period ranging from 30–42 weeks).

The $APC^{-}/PTEN^{-}$ tumors showed morphological similarity to human OEAs, with formation of distinct glands and occasional foci of squamous differentiation (Figures 4A–4D). As expected for tumors with epithelial differentiation, immunohistochemical staining for cytokeratins 8 and 19 was strongly positive in the tumor cells (Figures 4E and 4F). In 6 of 29 animals, peritoneal dissemination of tumor was manifested by tumor implants on the liver serosa (Figures 4G and 4H). Perivascular tumor within the liver parenchyma of these mice was occasionally observed. Also, as anticipated, the murine tumors that developed in the setting of *Apc* and *Pten* inactivation showed nuclear accumulation of β-catenin protein but lacked detectable expression of PTEN (Figures 5A and 5B). Similar to the tumors developing in the setting of K-RAS activation and PTEN inactivation described by Dinulescu et al. (hereafter referred to as $K\text{-}RAS^{mut}/PTEN^{-}$ tumors) the $APC^{-}/PTEN^{-}$ tumors showed increased pS6 staining, indicative of activated signaling through AKT (Figure 5C). The $APC^{-}/PTEN^{-}$ tumors also showed significant areas of less differentiated mesenchymal-appearing cells with vague spindle-cell morphology (Figures 5D and 5E). These areas are negative for cytokeratins (Figure 5F) and showed loss of E-cadherin immunoreactivity (Figure 5G) compared to portions of the tumor with glandular differentiation, suggesting epithelial-mesenchymal transition. Activated

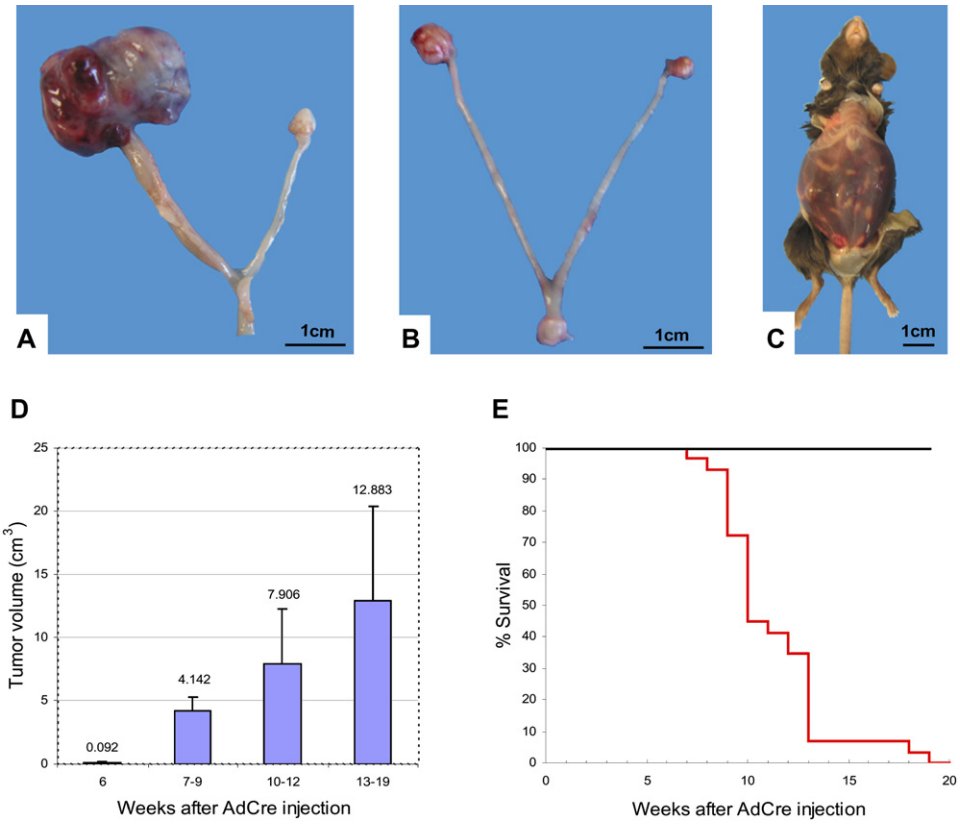

Figure 3. Inactivation of *Apc* and *Pten* in the Ovarian Surface Epithelium Induces Ovarian Carcinomas

(A) Female genital tract from *Apc*$^{loxP/loxP}$*Pten*$^{loxP/loxP}$ mouse 11 weeks after ovarian bursal AdCre injection. The right (injected) ovary shows a large, hemorrhagic tumor mass.

(B) Female genital tract from *Apc*$^{loxP/loxP}$*Pten*$^{loxP/loxP}$ 6 weeks after AdCre injection. Note the small tumor present in the right (injected) ovary.

(C) Representative mouse with carcinoma showing massive abdominal distension by hemorrhagic ascites.

(D) Tumor growth curve shows that tumor size doubles roughly every 3 weeks; bars indicate mean ± SD.

(E) Survival of *Apc*$^{loxP/loxP}$*Pten*$^{loxP/loxP}$ mice (red, n = 29) following AdCre injection versus wild-type control mice (black, n = 33).

Wnt/β-cat and PI3K/Pten signaling have both been implicated in epithelial-mesenchymal transition, a process thought to contribute to increased invasiveness and metastatic potential during tumor progression (reviewed by Larue and Bellacosa, 2005) (Brabletz et al., 2005). The mesenchymal-appearing areas do not likely represent malignant transformation of gonadal stroma (such as granulosa cell tumor), since they failed to express inhibin, a marker of gonadal stromal differentiation (Figure 4H). Moreover, we have examined several *ROSA26* reporter mice after ovarian bursal injection of AdCre and never observed β-galactosidase activity in ovarian stromal or other nonepithelial cells.

Comparison of Gene Expression in the APC^{-}/PTEN^{-} Murine Tumors to Human Ovarian Carcinomas Shows Greatest Similarity of the Mouse Tumors to Human OEAs with Deregulation of Wnt/β-catenin and/or PI3K/Pten Signaling

As described above, we used Affymetrix U133A oligonucleotide arrays to generate comprehensive gene expression data from 99 primary human ovarian carcinomas including all four of the major histologic types. We also profiled gene expression in four human ovaries incidentally removed from premenopausal women. Seven snap-frozen mouse APC^{-}/PTEN^{-} ovarian tumors 9 weeks after AdCre injection and eight contralateral (normal uninfected)/control ovaries from *Apc*$^{loxP/loxP}$*Pten*$^{loxP/loxP}$ mice were collected for use in gene expression-profiling experiments. mRNA was extracted from mouse tumor and whole normal ovary samples using the same methods we successfully employed previously for human tumor tissues. In order to obtain sufficient mRNA from the small normal mouse ovary specimens, normal ovary samples were combined into four groups of two samples each. We opted to compare gene expression in the tumors to that in whole normal ovary rather than ovarian surface epithelium because it is not possible to obtain sufficient quantities of nonneoplastic OSE for expression profiling without prior expansion of the cell population in culture, or alternatively, linear amplification of RNA isolated by laser capture microdissection before preparation of labeled cRNA. The normal mouse and human ovary samples serve as a common reference point for comparison of

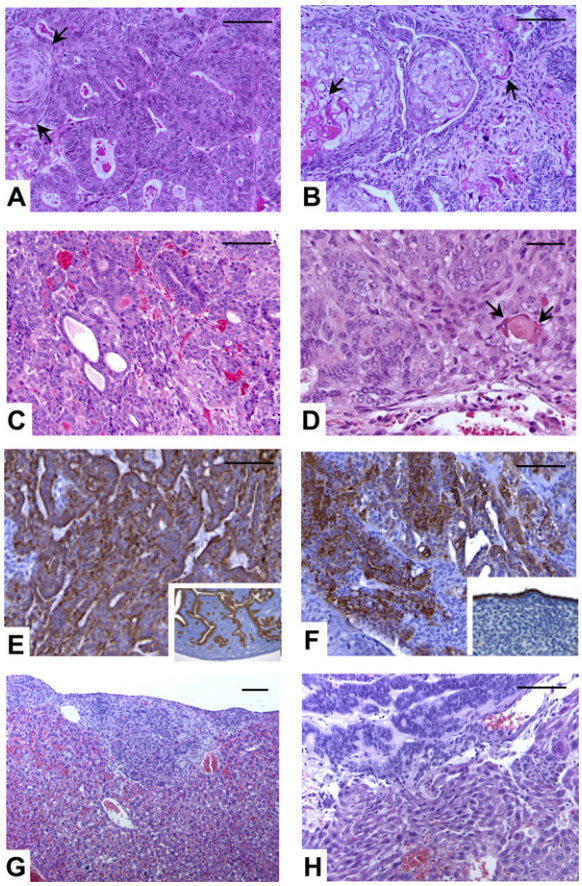

Figure 4. Murine Tumors Arising in *Apc*$^{loxP/loxP}$*Pten*$^{loxP/loxP}$ Animals Resemble Human OEAs with Respect to Morphology, Immunophenotype, and Biological Behavior

(A) Human OEA showing distinct gland formation and focal squamous differentiation (arrows). (B) Human OEA showing prominent squamous differentiation with focal keratinization (arrows). Mouse OEA-like tumor showing gland formation (C) and focal squamous differentiation (D) (arrows). Immunostains for cytokeratin 8 (E) (inset shows normal endometrium as positive control) and cytokeratin 19 (F) (inset shows normal ovarian surface epithelium as positive control) confirm epithelial differentiation of the tumor cells. A subset of animals showed dissemination of tumor on peritoneal surfaces, especially the liver serosa (G and H). Scale bars, 100 μm in (A)–(C) and (E)–(H), 40 μm in (D).

gene expression in tumors from mouse and human, respectively. Having a reference point with which to compare the tumor gene expression is essential because comparable hybridization of mouse and human cRNAs to probe sets representing homologous genes in the mouse and human cannot be assumed. The values obtained for each gene for these common control samples serve to calibrate the assays on the two arrays, compensating for possible differences in the affinities of the probes to their target sequences or the efficiency with which labeled cDNA is produced from the initial RNA samples.

Principal component analysis determined that the mouse tumor and normal ovary samples are easily separable based on global gene expression profile (data not shown). A similar analysis was performed for the human normal ovaries and ovarian carcinomas profiled on Affymetrix U133A arrays. Comparison of the seven mouse tumors and four normal pooled ovary samples identified 1088 probe sets with $p < 0.001$ and a minimum of 5-fold differences between tumor and normal (608 increased in tumors; 480 decreased). In order to estimate how many of these differences are likely false positives, we used the same selection criteria on 1000 data sets in which the sample labels were randomly permuted and obtained only 6.6 probe sets on average. Consequently, the estimated false discovery rate is excellent, at 0.61%.

The 1088 probe sets selected from the mouse data represent 774 distinct genes, 486 of which have orthologs represented on the human arrays. We correlated the average tumor-normal differences in log expression for these 486 mouse genes with the corresponding human genes' tumor-normal differences for each of the 99 human tumor samples. All correlations were positive (Table S2), ranging from 0.21 to 0.37, with the exception of a mucinous tumor with a correlation of 0.16. Ranking correlations from all four groups of human tumors gave average ranks of 61.1, 53.8, 42.6, and 30.1 for endometrioid, mucinous, serous, and clear-cell tumors, respectively. Endometrioid had higher-ranking correlations than clear cell ($p = 0.0066$, rank-sum test) and serous tumors ($p = 0.0041$); however, the difference between endometrioid and mucinous tumors was not significant ($p = 0.48$).

Notably, of the 99 human ovarian tumors with associated microarray-based expression data, 10 of the 13 human ovarian tumors most highly correlated to the mouse tumors' data were endometrioid, including the top six (Figure 6A and Table S2). Four of these six OEAs contained mutant β-catenin (OE-13T, -18T, -48T, and -55T), three of which also had mutations of *PTEN* (OE-13T, -48T, and -55T) and/or *PIK3CA* (OE-55T). These mutations, which deregulate the Wnt/β-cat and PI3K/Pten signaling pathways, likely cause a subset of the human tumors to be more correlated to the mouse tumors. Other highly correlated human tumors may also harbor mutations that deregulate Wnt/β-cat and PI3K/Pten signaling, although we have not yet collected these mutational data on the nonendometrioid cancers. The significantly higher correlations of OEAs as a group is most probably due to the greater frequency of tumors with such mutations in this group compared to the other histological types of ovarian carcinomas. We then compared the correlations of several subsets of endometrioid tumors defined by *CTNNB1/APC* mutation status or β-catenin immunohistochemical staining pattern using two-sided rank-sum tests, the results of which are shown in Figure 6B. Tumors with *CTNNB1* or *APC* mutations had higher correlations to the mouse tumor profile ($p = 0.0044$), as did tumors exhibiting nuclear accumulation of β-catenin ($p = 0.0011$). Low-stage (1 and 2) tumors had higher correlations than higher-stage (3 and 4) tumors ($p = 0.0003$).

We conclude that our mouse model of ovarian cancer, based on conditional deletion of *Apc* and *Pten*, shows morphological features, biological behavior, and gene

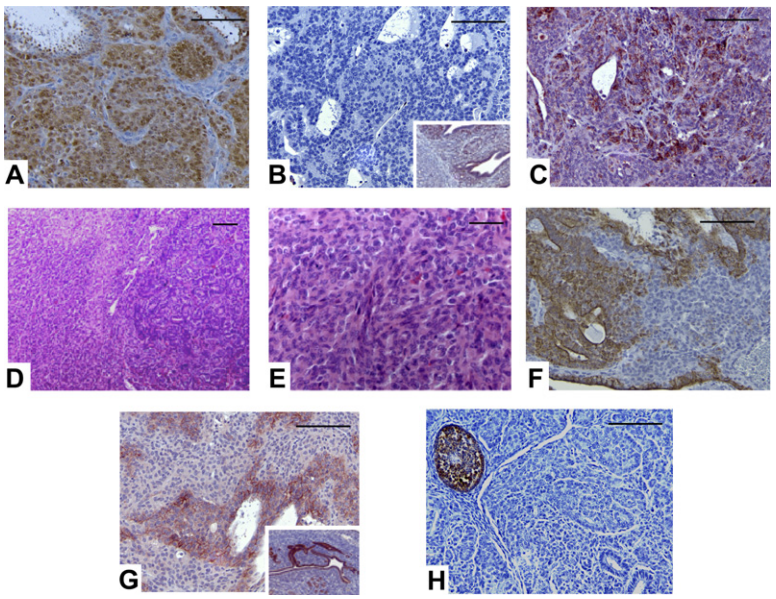

Figure 5. Murine APC^{-}/PTEN^{-} OEA-Like Tumors Show Evidence of Deregulated Wnt/β-cat and PI3K/Pten Signaling and Changes Suggestive of Epithelial-Mesenchymal Transition

Representative mouse tumor shows nuclear accumulation of β-catenin protein (A), loss of PTEN expression (B) (inset: normal mouse endometrium as positive control), and increased expression of pS6 (C). (D) Areas of tumor with spindle cell morphology (left) admixed with recognizable glandular elements (right) were often observed. These spindle cell areas (higher magnification in [E]) showed loss of cytokeratin 8 (F) and E-cadherin (G) expression, suggestive of epithelial-mesenchymal transition. An immunostain for inhibin (H), a marker of gonadal stromal differentiation, is negative in the tumor cells (note inhibin-positive follicular cells in upper left). Scale bars, 100 μm in (A)–(D) and (F)–(H), 40 μm in (E).

expression profiles similar to human cancers with the same signaling pathway defects.

DISCUSSION

Ovarian carcinomas are a morphologically heterogeneous group of tumors that can be divided into four major types based on their features when viewed by light microscopy. A number of characteristic genetic alterations have been identified in ovarian carcinomas, though the frequency with which a given gene is mutated varies substantially among the different subtypes (Bell, 2005). As our understanding of the molecular defects in ovarian cancer becomes more complete, characterization of the specific mutations in each individual tumor will likely be more informative than knowledge of the average behavior of the histological type to which the tumor belongs. Clearly, such specific information would aid in the design and use of effective drugs that target the particular molecular defects of the cancer cells. OEAs are the second most common

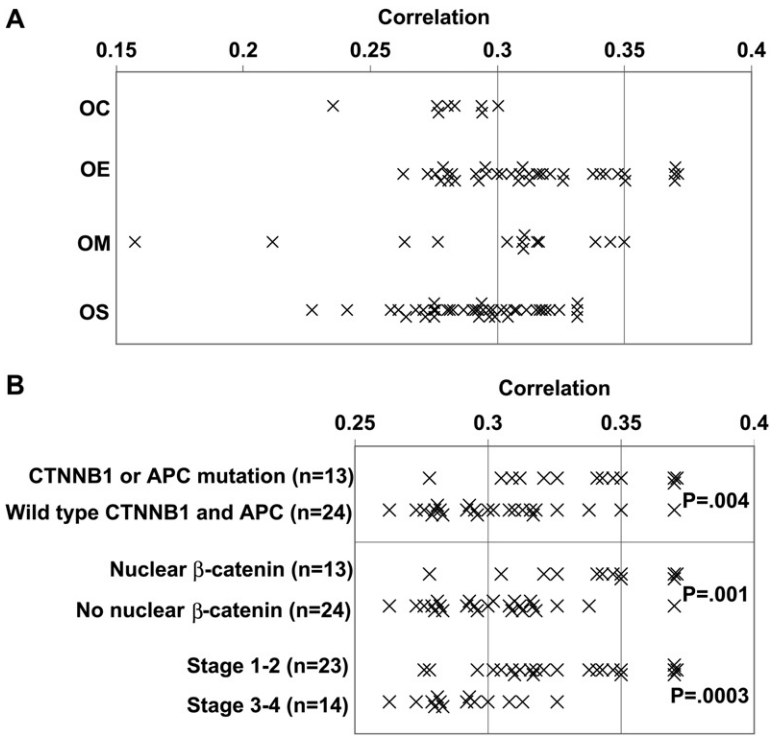

Figure 6. Gene Expression Profiling of Murine OEA-Like Tumors and Human Ovarian Carcinomas

(A) Correlation of differences from normal for genes altered in APC^{-}/PTEN^{-} murine tumors compared to groups of human ovarian carcinomas (OC, clear cell; OE, endometrioid; OM, mucinous; OS, serous).

(B) Correlations of mouse tumors to several subsets of human OEAs defined by *CTNNB1*/*APC* mutation status, β-catenin staining pattern, and stage (p values from two-sided rank-sum tests).

type of ovarian carcinoma, after serous carcinomas. We examined a large number of human OEAs to search for concomitant mutational defects in selected signaling pathways. We found a statistically significant correlation between defects in Wnt/β-cat and PI3K/Pten signaling. Indeed, two-thirds of OEAs with *PTEN* mutations also have Wnt/β-cat pathway defects. The OEAs with mutations predicted to deregulate Wnt/β-cat and/or PI3K/Pten signaling are typically low grade and distinguishable from the high-grade OEAs, which have a high prevalence of p53 mutations. Based on co-occurrence of these pathway defects in a subset of primary human OEAs, we investigated whether these signal transduction cascades work together to promote transformation in an in vivo model of ovarian cancer. The murine tumors that arise in the setting of *Apc* and *Pten* inactivation have similar histological features and gene expression profiles to their human OEA counterparts with comparable Wnt/β-cat and PI3K/Pten signaling pathway defects. All $Apc^{loxp/loxp}Pten^{loxP/loxP}$ mice developed tumors in the ovary injected with AdCre but not in the contralateral, uninjected ovary. Disease progression in these mice following AdCre injection is rapid and similar to that observed in women with untreated ovarian cancer, with frequent development of hemorrhagic ascites and peritoneal dissemination of tumor.

Although mice with ovarian epithelial-specific activation of K-RAS and inactivation of PTEN also develop tumors histologically resembling human OEAs (Dinulescu et al., 2005), our data indicate that activating *K-RAS* and inactivating *PTEN* mutations rarely if ever coexist in human OEAs. As such, the $APC^{-}/PTEN^{-}$ murine tumors may offer a useful complement to the $K\text{-}RAS^{mut}/PTEN^{-}$ tumors for studying the biology of OEAs and for preclinical testing of molecularly targeted therapeutics likely to be effective in treating human OEAs. Notably, however, the tumors arising in the $Apc^{loxP/loxP}Pten^{loxP/loxP}$ mice are not accompanied by endometriosis. Dinulescu and colleagues found that endometriosis-like lesions often developed after ovarian bursal injection of AdCre allowing activation of an oncogenic *K-ras* allele. This is an intriguing observation, since the association of endometriosis with both endometrioid and clear-cell ovarian adenocarcinomas has long been recognized (Fukunaga et al., 1997; Erzen et al., 2001). Despite this association, data supporting endometriosis as an obligate precursor of OEA are lacking, and the role of oncogenic K-ras in the pathogenesis of endometriosis remains uncertain. Indeed, several studies failed to identify *K-RAS* mutations in human endometriotic lesions (Vercellini et al., 1994; Amemiya et al., 2004; Otsuka et al., 2004). Dinulescu and colleagues proposed that alternative mechanisms of RAS pathway activation may be involved in the development of endometriosis. In any event, Wnt/β-cat signaling pathway activation does not appear to be directly related to endometriosis, at least in our mouse model. We have not identified β-catenin mutations in human endometriotic lesions in the absence of endometrioid adenocarcinoma (Y.Z., R.W., and K.R.C., unpublished data).

The mechanism for synergistic effects of activating the PI3K/Pten and Wnt/β-cat signaling pathways in this model is unclear at this point. Akt has a number of substrates, one of which is GSK3β. However, Akt's ability to negatively regulate GSK3β's activity on β-catenin remains uncertain (Yuan et al., 1999), and mutant β-catenin alleles are resistant to regulation by GSK3β. Some studies suggest the GSK3β pools associated with the Wnt and PI3K/Pten pathways are distinct, while others suggest these pools are not mutually exclusive and may interact to mediate effects of upstream growth factor activators (reviewed by Mulholland et al., 2006). Recently, Wnt has been shown to activate mTOR (a downstream effector of activated Akt) via inhibition of GSK3β, but without involving β-catenin-dependent transcription (Inoki et al., 2006). Hence, while the two pathways intersect, the mechanisms for their cooperation in cancer pathogenesis are not obvious.

As indicated above, either activation of K-RAS or deregulation of β-catenin can cooperate with AKT activation in mouse models of ovarian carcinoma. Notably, activation of Akt is one of the most common occurrences in human cancer. One model postulated to explain this is that activated Akt upregulates glycolysis, which is thought to be required to support the high rate of cancer cell proliferation (Bui and Thompson, 2006; Thompson and Thompson, 2004). Several studies have found that deregulated PI3K/Pten signaling is a major determinant of cell growth and survival in many cancer types, and a number of small molecules targeting the upstream and downstream components of this pathway have been developed (reviewed by Powis et al., 2006 and Granville et al., 2006). Given the importance of PI3K/Pten signaling in regulating the growth properties of normal cells, as well as the complexity of its regulation, it may be difficult to identify efficacious anticancer drugs with acceptably low toxicity. However, recent work showing that inhibition of mTOR by treatment with rapamycin can inhibit the growth of Pten-deficient leukemia cells while restoring hematopoietic stem cell growth (Yilmaz et al., 2006) suggests that such agents can be identified. Whether rapamycin has similar effects on the $APC^{-}/PTEN^{-}$ murine tumors is under investigation. Animal models that can be used to test PI3K/Pten pathway inhibitors, alone and in combination, will likely prove particularly useful in the development of new therapeutics.

Although development of Wnt signaling pathway inhibitors as cancer therapeutics is not as far advanced as that for PI3K signaling, some small molecules antagonizing the interaction of β-catenin with key nuclear proteins have been identified (Lepourcelet et al., 2004; Emami et al., 2004; Janssens et al., 2006). The observation that canonical Wnt signaling also upregulates the activity of mTOR (Inoki et al., 2006) provides further impetus for testing effects of rapamycin and its analogs in this model system. The $APC^{-}/PTEN^{-}$ murine ovarian tumors described here have similar genetic defects, morphology, and clinical behavior to their human OEA counterparts, and this model of OEA should prove useful in evaluating both chemopreventive and chemotherapeutic strategies for ovarian cancer.

EXPERIMENTAL PROCEDURES

Human Tumor Samples

Seventy-two snap-frozen OEA samples were analyzed for mutations of *CTNNB1*, *K-RAS*, *PTEN*, *PIK3CA*, and *TP53*: 60 samples were from the Cooperative Human Tissue Network/Gynecologic Oncology Group Tissue Bank, 6 were from Johns Hopkins Hospital, 5 were from Kumamoto University Hospital, and 1 was from the University of Michigan Health System. OEAs were classified as well differentiated (grade 1, n = 18), moderately differentiated (grade 2, n = 26), or poorly differentiated (grade 3, n = 28) using FIGO criteria. FIGO criteria were also used to assign tumor stage (stage 1, n = 29; stage 2, n = 15; stages 3 and 4, n = 28). Primary tumor tissues were manually dissected with microscope guidance to ensure that each tumor sample contained a minimum of 70% tumor cells. Genomic DNA and RNA were isolated from pooled frozen tissue sections using standard techniques as we have described previously (Wu et al., 2001). Mutational analyses of *CTNNB1*, *K-RAS*, *PTEN*, *PIK3CA*, and *p53* were performed on all 72 OEAs using published and custom primer sequences (unpublished primer sequences provided upon request) (Wu et al., 2001; Oda et al., 2005). A small subset of OEAs with nuclear accumulation of β-catenin protein but lacking *CTNNB1* mutations were evaluated for *APC* mutations in a previously reported study (Wu et al., 2001). A set of 99 snap-frozen primary ovarian carcinomas were used for expression profiling, including 41 serous, 37 endometrioid, 13 mucinous, and 8 clear cell carcinomas. The 37 OEAs used for the expression profiling analysis were included in the mutational analysis of 72 OEAs described above. Analysis of tissues from human subjects was approved by the University of Michigan's Institutional Review Board (IRBMED protocols 1999-0428 and 2001-0568).

Immunohistochemical Staining of Human Tumors

Formalin-fixed, paraffin-embedded OEA tissues were immunohistochemically stained for β-catenin, Pten, pS6 ribosomal protein, and p53 using standard techniques. Methods for immunohistochemical analysis of β-catenin have been previously described (Zhai et al., 2002). Sections were immunostained using mouse monoclonal anti-Pten antibody (1:400, Clone 6H2.1, Cascade Biosciences, Winchester, MA), mouse monoclonal anti-p53 antibody (1:500, clone DO-7, Invitrogen, San Diego, CA), or rabbit polyclonal anti-pS6 ribosomal protein (1:500, clone 91B2, Cell Signaling Technology, Danvers, MA). Antigen-antibody complexes were detected with the avidin-biotin peroxidase method using NovaRed (Pten) or 3,3′-diaminobenzidine as a chromogenic substrate (β-catenin, pS6, p53) (Vectastain ABC kit; Vector Laboratories, Burlingame, CA). Immunostaining for Pten and nuclear β-catenin was scored on a three-tiered scale for intensity (−, absent; +, retained; ++, strongly retained) in the epithelial portions of tumor sections compared to the stromal components. Immunostaining for nuclear accumulation of p53 was scored as negative (absent or weak/focal) or positive (strong and diffuse).

Mouse Strains

$Apc^{loxP/loxP}$ mice and $Pten^{loxP/loxP}$ mice have been previously described in detail (Shibata et al., 1997; Suzuki et al., 2001). $Apc^{loxP/loxP}Pten^{loxP/loxP}$ mice were generated by crossbreeding $Apc^{loxP/loxP}$ with $Pten^{loxP/loxP}$ mice. The genotype of each strain was confirmed by PCR using tail biopsy DNA and primer sequences described previously (Backman et al., 2001; Shibata et al., 1997). *Gt(ROSA)26Sor* reporter mice (R26R) were purchased from Jackson Laboratories (Bar Harbor, ME) (Soriano, 1999). All animal procedures were approved by the University of Michigan's Committee on Use and Care of Animals (UCUCA, protocol #8742).

Ovarian Tumor Development after Intrabursal Injection of Adenovirus Expressing Cre Recombinase

Replication-incompetent recombinant adenovirus expressing Cre recombinase under the control of the CMV promoter (AdCre) (Anton and Graham, 1995) was obtained from University of Michigan's Vector Core. Plaque-forming units (pfu; 5×10^7) of AdCre with 0.1% Evans blue (Sigma-Aldrich Inc., St. Louis, MO) in a total volume of 5 μl was injected into the right ovarian bursal cavity of 56- to 70-day-old female mice. A 32-gauge needle was introduced into the oviduct near the infundibulum and into the ovarian bursa as described previously (Flesken-Nikitin et al., 2003; Dinulescu et al., 2005). The left ovarian bursa was not injected and served as a normal control. A total of 80 $Apc^{loxP/loxP}$, 70 $Pten^{loxP/loxP}$, 50 $Apc^{loxP/loxP}/Pten^{loxP/loxP}$, and 40 C57BL6 wild-type mice underwent intrabursal injection of AdCre. Localization of Cre expression to the ovarian surface epithelium after intrabursal injection of AdCre was evaluated in R26R reporter mice. Seventy-two hours after a single intrabursal injection of AdCre, reporter mice were euthanized and the female genital tract, liver, kidneys, spleen, digestive tract, lungs, and heart were harvested and fixed in 4% paraformaldehyde for 20 min, then stained in X-gal (Invitrogen) solution for 2 hr at 37°C. After staining, tissues were postfixed in 4% paraformaldehyde, dehydrated in 30% sucrose, and embedded in OCT compound. Frozen sections were counterstained with nuclear fast red (Sigma-Aldrich Inc.). Following AdCre injection, all $Apc^{loxP/loxP}$, $Pten^{loxP/loxP}$, $Apc^{loxP/loxP}/Pten^{loxP/loxP}$, and wild-type mice were monitored at least twice weekly until palpable tumors were detected, and daily after tumor formation was evident. Twenty-nine mice died spontaneously or were euthanized by CO_2 asphyxiation when clinical signs of morbidity associated with tumor burden were identified, in compliance with the institutional guidelines. A subset of $Apc^{loxP/loxP}/Pten^{loxP/loxP}$ mice were euthanized 6 weeks after AdCre injection to determine if ovarian tumors were present at this time point. Another subset of $Apc^{loxP/loxP}/Pten^{loxP/loxP}$ mice were euthanized 9 weeks after injection to obtain tumors for gene expression profiling studies. Genomic DNA from tumors was prepared as previously described (Wu et al., 2001). PCR was performed using mouse tumor and normal DNA to validate Cre-mediated recombination of *Apc* and *Pten* alleles.

Mouse Tissue Histopathology

All mice were examined at necropsy for gross organ abnormalities. The genital system, liver, lungs, spleen, kidney, brain, and digestive tract were collected, fixed in 10% (v/v) buffered formalin, and embedded in paraffin for histopathological evaluation. Histopathological evaluation of tumor and other tissues was performed by a surgical pathologist with expertise in ovarian cancer diagnosis (K.R.C.).

Immunohistochemical Staining of Mouse Tumor Tissues

Immunohistochemical staining was performed on formalin-fixed, paraffin-embedded tissue sections using standard methods. For mouse primary monoclonal antibodies (anti-β-catenin, 1:500, Transduction Laboratories, Lexington, KY; and anti-inhibin, 1:50, Serotac Ltd, Oxford, UK), the Mouse on Mouse kit (M.O.M., Vector laboratories) was used to reduce nonspecific staining per the manufacturer's instructions. Rat monoclonal antibodies to CK8 (TROMAI, 1:10) and CK19 (TROMAIII, 1:10) were obtained from the Developmental Studies Hybridoma Bank (The University of Iowa, Iowa City, IA). Other antibodies employed included anti-E-cadherin (1:200, clone ECCD-2, Zymed, South San Francisco, CA), anti-PTEN (1:100, clone 138G6, Cell Signaling Technology), anti-pS6 (1:100, clone 91B2, Cell Signaling Technology), and biotinylated rabbit anti-rat IgG (BA-4001, Vector Laboratories).

Gene Expression Profiling

Frozen mouse tumor tissues were manually microdissected before RNA extraction to ensure that each tumor sample contained at least 90% neoplastic cells in tumor samples. Matched normal ovaries were used for controls. RNA isolation and cRNA synthesis were performed as previously described (Schwartz et al., 2002). cRNAs were hybridized to GeneChip Mouse Genome 430 2.0 Arrays (Affymetrix, Santa Clara, CA). The arrays were scanned using Affymetrix Scanner 3000. Image analysis was performed with GeneChip software (Affymetrix). Human tumor and ovary samples were hybridized to U133A Arrays (Affymetrix).

Gene Expression Data Analysis

Array hybridization, scanning, and image analysis, using Human Genome U133A arrays with 22283 probe sets, were performed according to the manufacturer's protocols (Affymetrix, Santa Clara, CA). Probeset intensities were obtained and normalized as previously described, using publicly available software (Giordano et al., 2001). Mouse samples and arrays were processed using methods identical to those used for human tissues, except that Mouse430_2 arrays with 45,101 probe sets were used, and the probe-set intensities were scaled to give an average of 1000 rather than 1500 units. Data were log transformed using $Y = \log(\max(x + 50,0) + 50)$ for both the mouse and human data sets, and all subsequent analysis used only the transformed data. Fold changes between groups of samples were based on the averages of the transformed data. The array data are available from NCBI's Gene Expression Omnibus (GEO, http://www.ncbi.nlm.nih.gov/geo/) using series accession numbers GSE6008 (human arrays) and GSE5987 (mouse arrays). Annotations indicating the gene represented by each probe set as of December 19, 2005, were obtained from Affymetrix web sites for both human and mouse arrays. Mouse genes were joined to human homologs using downloads of Homologene from NCBI web sites, obtained January 12, 2006.

Supplemental Data

The Supplemental Data include two supplemental tables and can be found with this article online at http://www.cancercell.org/cgi/content/full/11/4/321/DC1/.

ACKNOWLEDGMENTS

The authors wish to thank Kit Yuen, Heather Reed, Jonathan Dunker, and Lisa So for technical assistance and Thom Saunders of the University of Michigan Medical School's transgenic animal model core for assistance with ovarian bursal injections. The authors also thank Drs. Tak Mak and Tetsuo Noda for providing access to the Pten-flox and Apc-flox mice used in this project. This work was supported by funds from the National Cancer Institute, NIH (P30 CA46592, U19 CA84953, RO1 CA94172, and RO1 CA85463) and from the Department of Defense (W81WH-04-1-0211).

Received: October 9, 2006
Revised: January 5, 2007
Accepted: February 21, 2007
Published: April 9, 2007

REFERENCES

Altomare, D.A., and Testa, J.R. (2005). Perturbations of the AKT signaling pathway in human cancer. Oncogene *24*, 7455–7464.

Amemiya, S., Sekizawa, A., Otsuka, J., Tachikawa, T., Saito, H., and Okai, T. (2004). Malignant transformation of endometriosis and genetic alterations of K-ras and microsatellite instability. Int. J. Gynaecol. Obstet. *86*, 371–376.

Anton, M., and Graham, F.L. (1995). Site-specific recombination mediated by an adenovirus vector expressing the Cre recombinase protein: A molecular switch for control of gene expression. J. Virol. *69*, 4600–4606.

Backman, S.A., Stambolic, V., Suzuki, A., Haight, J., Elia, A., Pretorius, J., Tsao, M.S., Shannon, P., Bolon, B., Ivy, G.O., and Mak, T.W. (2001). Deletion of Pten in mouse brain causes seizures, ataxia and defects in soma size resembling Lhermitte-Duclos disease. Nat. Genet. *29*, 396–403.

Baeza, N., Weller, M., Yonekawa, Y., Kleihues, P., and Ohgaki, H. (2003). PTEN methylation and expression in glioblastomas. Acta Neuropathol. (Berl.) *106*, 479–485.

Bell, D.A. (2005). Origins and molecular pathology of ovarian cancer. Mod. Pathol. *18* (*Suppl 2*), S19–S32.

Brabletz, T., Hlubek, F., Spaderna, S., Schmalhofer, O., Hiendlmeyer, E., Jung, A., and Kirchner, T. (2005). Invasion and metastasis in colorectal cancer: Epithelial-mesenchymal transition, mesenchymal-epithelial transition, stem cells and beta-catenin. Cells Tissues Organs *179*, 56–65.

Brachtel, E.F., Sanchez-Estevez, C., Moreno-Bueno, G., Prat, J., Palacios, J., and Oliva, E. (2005). Distinct molecular alterations in complex endometrial hyperplasia (CEH) with and without immature squamous metaplasia (squamous morules). Am. J. Surg. Pathol. *29*, 1322–1329.

Bui, T., and Thompson, C.B. (2006). Cancer's sweet tooth. Cancer Cell *9*, 419–420.

Caduff, R.F., Svoboda-Newman, S.M., Bartos, R.E., Ferguson, A.W., and Frank, T.S. (1998). Comparative analysis of histologic homologues of endometrial and ovarian carcinoma. Am. J. Surg. Pathol. *22*, 319–326.

Campbell, I.G., and Thomas, E.J. (2001). Endometriosis: Candidate genes. Hum. Reprod. Update *7*, 15–20.

Campbell, I.G., Russell, S.E., Choong, D.Y., Montgomery, K.G., Ciavarella, M.L., Hooi, C.S., Cristiano, B.E., Pearson, R.B., and Phillips, W.A. (2004). Mutation of the PIK3CA gene in ovarian and breast cancer. Cancer Res. *64*, 7678–7681.

Catasus, L., Bussaglia, E., Rodrguez, I., Gallardo, A., Pons, C., Irving, J.A., and Prat, J. (2004). Molecular genetic alterations in endometrioid carcinomas of the ovary: Similar frequency of beta-catenin abnormalities but lower rate of microsatellite instability and PTEN alterations than in uterine endometrioid carcinomas. Hum. Pathol. *35*, 1360–1368.

Cheng, W., Liu, J., Yoshida, H., Rosen, D., and Naora, H. (2005). Lineage infidelity of epithelial ovarian cancers is controlled by HOX genes that specify regional identity in the reproductive tract. Nat. Med. *11*, 531–537.

Connolly, D.C., Bao, R., Nikitin, A.Y., Stephens, K.C., Poole, T.W., Hua, X., Harris, S.S., Vanderhyden, B.C., and Hamilton, T.C. (2003). Female mice chimeric for expression of the simian virus 40 TAg under control of the MISIIR promoter develop epithelial ovarian cancer. Cancer Res. *63*, 1389–1397.

Cuatrecasas, M., Villanueva, A., Matias-Guiu, X., and Prat, J. (1997). K-ras mutations in mucinous ovarian tumors: A clinicopathologic and molecular study of 95 cases. Cancer *79*, 1581–1586.

Dinulescu, D.M., Ince, T.A., Quade, B.J., Shafer, S.A., Crowley, D., and Jacks, T. (2005). Role of K-ras and Pten in the development of mouse models of endometriosis and endometrioid ovarian cancer. Nat. Med. *11*, 63–70.

Emami, K.H., Nguyen, C., Ma, H., Kim, D.H., Jeong, K.W., Eguchi, M., Moon, R.T., Teo, J.L., Kim, H.Y., Moon, S.H., et al. (2004). A small molecule inhibitor of beta-catenin/CREB-binding protein transcription. Proc. Natl. Acad. Sci. USA *101*, 12682–12687.

Enomoto, T., Weghorst, C.M., Inoue, M., Tanizawa, O., and Rice, J.M. (1991). K-ras activation occurs frequently in mucinous adenocarcinomas and rarely in other common epithelial tumors of the human ovary. Am. J. Pathol. *139*, 777–785.

Erzen, M., Rakar, S., Klancnik, B., Syrjanen, K., and Klancar, B. (2001). Endometriosis-associated ovarian carcinoma (EAOC): an entity distinct from other ovarian carcinomas as suggested by a nested case-control study. Gynecol. Oncol. *83*, 100–108.

Flesken-Nikitin, A., Choi, K.C., Eng, J.P., Shmidt, E.N., and Nikitin, A.Y. (2003). Induction of carcinogenesis by concurrent inactivation of p53 and Rb1 in the mouse ovarian surface epithelium. Cancer Res. *63*, 3459–3463.

Fukunaga, M., Nomura, K., Ishikawa, E., and Ushigome, S. (1997). Ovarian atypical endometriosis: Its close association with malignant epithelial tumours. Histopathology *30*, 249–255.

Gamallo, C., Palacios, J., Moreno, G., Calvo de Mora, J., Suarez, A., and Armas, A. (1999). beta-catenin expression pattern in stage I and

II ovarian carcinomas: Relationship with beta-catenin gene Mutations, Clinicopathological features, and clinical outcome. Am. J. Pathol. *155*, 527–536.

Giordano, T.J., Shedden, K.A., Schwartz, D.R., Kuick, R., Taylor, J.M.G., Lee, N., Misek, D.E., Greenson, J.K., Kardia, S.L.R., Beer, D.G., Rennert, G., Cho, K.R., Gruber, S.B., Fearon, E.R., and Hanash, S. (2001). Organ-specific molecular classification of primary lung, colon, and ovarian adenocarcinomas using gene expression profiles. Am. J. Pathol. *159*, 1231–1238.

Granville, C.A., Memmott, R.M., Gills, J.J., and Dennis, P.A. (2006). Handicapping the race to develop inhibitors of the phosphoinositide 3-kinase/Akt/mammalian target of rapamycin pathway. Clin. Cancer Res. *12*, 679–689.

Guppy, A.E., Nathan, P.D., and Rustin, G.J. (2005). Epithelial ovarian cancer: A review of current management. Clin. Oncol. (R Coll Radiol) *17*, 399–411.

Han, S.Y., Kato, H., Kato, S., Suzuki, T., Shibata, H., Ishii, S., Shiiba, K., Matsuno, S., Kanamaru, R., and Ishioka, C. (2000). Functional evaluation of PTEN missense mutations using in vitro phosphoinositide phosphatase assay. Cancer Res. *60*, 3147–3151.

Ichikawa, Y., Nishida, M., Suzuki, H., Yoshida, S., Tsunoda, H., Kubo, T., Uchida, K., and Miwa, M. (1994). Mutation of K-ras protooncogene is associated with histological subtypes in human mucinous ovarian tumors. Cancer Res. *54*, 33–35.

Inoki, K., Ouyang, H., Zhu, T., Lindvall, C., Wang, Y., Zhang, X., Yang, Q., Bennett, C., Harada, Y., Stankunas, K., et al. (2006). TSC2 integrates Wnt and energy signals via a coordinated phosphorylation by AMPK and GSK3 to regulate cell growth. Cell *126*, 955–968.

Janssens, N., Janicot, M., and Perera, T. (2006). The Wnt-dependent signaling pathways as target in oncology drug discovery. Invest. New Drugs *24*, 263–280.

Kato, H., Kato, S., Kumabe, T., Sonoda, Y., Yoshimoto, T., Kato, S., Han, S.Y., Suzuki, T., Shibata, H., Kanamaru, R., and Ishioka, C. (2000). Functional evaluation of p53 and PTEN gene mutations in gliomas. Clin. Cancer Res. *6*, 3937–3943.

Kildal, W., Risberg, B., Abeler, V.M., Kristensen, G.B., Sudbo, J., Nesland, J.M., and Danielsen, H.E. (2005). beta-catenin expression, DNA ploidy and clinicopathological features in ovarian cancer: A study in 253 patients. Eur. J. Cancer *41*, 1127–1134.

Kolasa, I.K., Rembiszewska, A., Janiec-Jankowska, A., Dansonka-Mieszkowska, A., Lewandowska, A.M., Konopka, B., and Kupryjanczyk, J. (2006). PTEN mutation, expression and LOH at its locus in ovarian carcinomas. Relation to TP53, K-RAS and BRCA1 mutations. Gynecol. Oncol. *103*, 692–697.

Larue, L., and Bellacosa, A. (2005). Epithelial-mesenchymal transition in development and cancer: Role of phosphatidylinositol 3′ kinase/AKT pathways. Oncogene *24*, 7443–7454.

Lepourcelet, M., Chen, Y.N., France, D.S., Wang, H., Crews, P., Petersen, F., Bruseo, C., Wood, A.W., and Shivdasani, R.A. (2004). Small-molecule antagonists of the oncogenic Tcf/beta-catenin protein complex. Cancer Cell *5*, 91–102.

Moreno-Bueno, G., Gamallo, C., Perez-Gallego, L., de Mora, J.C., Suarez, A., and Palacios, J. (2001). β-catenin expression pattern, β-catenin gene mutations, and microsatellite instability in endometrioid ovarian carcinomas and synchronous endometrial carcinomas. Diagn. Mol. Pathol. *10*, 116–122.

Mulholland, D.J., Dedhar, S., Wu, H., and Nelson, C.C. (2006). PTEN and GSK3beta: Key regulators of progression to androgen-independent prostate cancer. Oncogene *25*, 329–337.

Nagy, A., Gertsenstein, M., Vintersten, K., and Behringer, R. (2003). Manipulating the Mouse Embryo: A Laboratory Manual (New York: Cold Spring Harbor Laboratory Press).

Obata, K., Morland, S.J., Watson, R.H., Hitchcock, A., Chenevix-Trench, G., Thomas, E.J., and Campbell, I.G. (1998). Frequent PTEN/MMAC mutations in endometrioid but not serous or mucinous epithelial ovarian tumors. Cancer Res. *58*, 2095–2097.

Oda, K., Stokoe, D., Taketani, Y., and McCormick, F. (2005). High frequency of coexistent mutations of PIK3CA and PTEN genes in endometrial carcinoma. Cancer Res. *65*, 10669–10673.

Orsulic, S., Li, Y., Soslow, R.A., Vitale-Cross, L.A., and Varmus, H.E. (2002). Induction of ovarian cancer by defined multiple genetic changes in a mouse model system. Cancer Cell *1*, 53–62.

Otsuka, J., Okuda, T., Sekizawa, A., Amemiya, S., Saito, H., Okai, T., Kushima, M., and Tachikawa, T. (2004). K-ras mutation may promote carcinogenesis of endometriosis leading to ovarian clear cell carcinoma. Med. Electron Microsc. *37*, 188–192.

Powis, G., Ihle, N., and Kirkpatrick, D.L. (2006). Practicalities of drugging the phosphatidylinositol-3-kinase/Akt cell survival signaling pathway. Clin. Cancer Res. *12*, 2964–2966.

Risinger, J.I., Hayes, K., Maxwell, G.L., Carney, M.E., Dodge, R.K., Barrett, J.C., and Berchuck, A. (1998). PTEN mutation in endometrial cancers is associated with favorable clinical and pathologic characteristics. Clin. Cancer Res. *4*, 3005–3010.

Sagae, S., Kobayashi, K., Nishioka, Y., Sugimura, M., Ishioka, S., Nagata, M., Terasawa, K., Tokino, T., and Kudo, R. (1999). Mutational analysis of beta-catenin gene in Japanese ovarian carcinomas: Frequent mutations in endometrioid carcinomas. Jpn. J. Cancer Res. *90*, 510–515.

Samuels, Y., Wang, Z., Bardelli, A., Silliman, N., Ptak, J., Szabo, S., Yan, H., Gazdar, A., Powell, S.M., Riggins, G.J., et al. (2004). High frequency of mutations of the PIK3CA gene in human cancers. Science *304*, 554.

Schuijer, M., and Berns, E.M. (2003). TP53 and ovarian cancer. Hum. Mutat. *21*, 285–291.

Schwartz, D.R., Kardia, S.L., Shedden, K.A., Kuick, R., Michailidis, G., Taylor, J.M., Misek, D.E., Wu, R., Zhai, Y., Darrah, D.M., et al. (2002). Gene expression in ovarian cancer reflects both morphology and biological behavior, distinguishing clear cell from other poor-prognosis ovarian carcinomas. Cancer Res. *62*, 4722–4729.

Scully, R.E., Young, R.H., and Clement, P.B. (1998). Tumors of the Ovary, Maldeveloped Gonads, Fallopian Tube, and Broad Ligament. Atlas of Tumor Pathology, Third Series, Fascicle 23 (Washington, D.C.: Armed Forces Institute of Pathology).

Shibata, H., Toyama, K., Shioya, H., Ito, M., Hirota, M., Hasegawa, S., Matsumoto, H., Takano, H., Akiyama, T., Toyoshima, K., et al. (1997). Rapid colorectal adenoma formation initiated by conditional targeting of the Apc gene. Science *278*, 120–123.

Sieben, N.L., Macropoulos, P., Roemen, G.M., Kolkman-Uljee, S.M., Jan Fleuren, G., Houmadi, R., Diss, T., Warren, B., Al Adnani, M., De Goeij, A.P., et al. (2004). In ovarian neoplasms, BRAF, but not KRAS, mutations are restricted to low-grade serous tumours. J. Pathol. *202*, 336–340.

Soriano, P. (1999). Generalized lacZ expression with the ROSA26 Cre reporter strain. Nat. Genet. *21*, 70–71.

Suzuki, A., Yamaguchi, M.T., Ohteki, T., Sasaki, T., Kaisho, T., Kimura, Y., Yoshida, R., Wakeham, A., Higuchi, T., Fukumoto, M., et al. (2001). T cell-specific loss of Pten leads to defects in central and peripheral tolerance. Immunity *14*, 523–534.

Tashiro, H., Blazes, M.S., Wu, R., Cho, K.R., Bose, S., Wang, S.I., Li, J., Parsons, R.E., and Ellenson, L.H. (1997). Mutations in PTEN are frequent in endometrial carcinoma but rare in other common gynecological malignancies. Cancer Res. *57*, 3935–3940.

Thomas, G.V., Horvath, S., Smith, B.L., Crosby, K., Lebel, L.A., Schrage, M., Said, J., De Kernion, J., Reiter, R.E., and Sawyers, C.L. (2004). Antibody-based profiling of the phosphoinositide 3-kinase pathway in clinical prostate cancer. Clin. Cancer Res. *10*, 8351–8356.

Thompson, J.E., and Thompson, C.B. (2004). Putting the rap on Akt. J. Clin. Oncol. *22*, 4217–4226.

Vercellini, P., Trecca, D., Oldani, S., Fracchiolla, N.S., Neri, A., and Crosignani, P.G. (1994). Analysis of p53 and ras gene mutations in endometriosis. Gynecol. Obstet. Invest. *38*, 70–71.

Vogelstein, B., and Kinzler, K.W. (2004). Cancer genes and the pathways they control. Nat. Med. *10*, 789–799.

Wright, K., Wilson, P., Morland, S., Campbell, I., Walsh, M., Hurst, T., Ward, B., Cummings, M., and Chenevix-Trench, G. (1999). beta-catenin mutation and expression analysis in ovarian cancer: Exon 3 mutations and nuclear translocation in 16% of endometrioid tumours. Int. J. Cancer *82*, 625–629.

Wu, R., Zhai, Y., Fearon, E.R., and Cho, K.R. (2001). Diverse Mechanisms of beta-Catenin Deregulation in Ovarian Endometrioid Adenocarcinomas. Cancer Res. *61*, 8247–8255.

Yilmaz, O.H., Valdez, R., Theisen, B.K., Guo, W., Ferguson, D.O., Wu, H., and Morrison, S.J. (2006). Pten dependence distinguishes haematopoietic stem cells from leukaemia-initiating cells. Nature *441*, 475–482.

Yuan, H., Mao, J., Li, L., and Wu, D. (1999). Suppression of glycogen synthase kinase activity is not sufficient for leukemia enhancer factor-1 activation. J. Biol. Chem. *274*, 30419–30423.

Zhai, Y., Wu, R., Schwartz, D.R., Darrah, D., Reed, H., Kolligs, F.T., Nieman, M.T., Fearon, E.R., and Cho, K.R. (2002). Role of beta-catenin/T-cell factor-regulated genes in ovarian endometrioid adenocarcinomas. Am. J. Pathol. *160*, 1229–1238.

Accession Numbers

The array data are available from NCBI's Gene Expression Omnibus (GEO, http://www.ncbi.nlm.nih.gov/geo/) using series accession numbers GSE6008 (human arrays) and GSE5987 (mouse arrays).